

A new multi-stable fractional-order four-dimensional system with self-excited and hidden chaotic attractors: Dynamic analysis and adaptive synchronization using a novel fuzzy adaptive sliding mode control method

Hadi Jahanshahi¹, Amin Yousefpour², Jesus M. Munoz-Pacheco³, Irene Moroz⁴, Zhouchao Wei⁵, Oscar Castillo⁶

¹Department of Aerospace Engineering, University of Tehran, Tehran, 14395 -1561, Iran.

²School of Mechanical Engineering, College of Engineering, University of Tehran, Tehran, 14399–57131, Iran.

³Faculty of Electronics Sciences, Benemerita Universidad Autonoma de Puebla, Mexico, 72570.

⁴Mathematical Institute, University of Oxford, Oxford, OX2 6GG, England, UK.

⁵School of Mathematics and Physics, China University of Geosciences, Wuhan, 430074, P. R. China.

⁶Division of Graduate Studies and Research, Tijuana Institute of Technology, Tijuana, Mexico

Abstract:

Four-dimensional chaotic systems are currently a very interesting topic for researchers, given their special features. This paper presents a novel fractional-order four-dimensional chaotic system with self-excited and hidden attractors, which includes only one constant term. The proposed system presents the phenomenon of multi-stability, which means that two or more different dynamics are generated from different initial conditions. It is one of few published works in the last five years belonging to the aforementioned category. Using Lyapunov exponents, the chaotic behaviour of the dynamical system is characterized, and the sensitivity of the system to initial conditions is determined. Also, systematic studies of the hidden chaotic behaviour in the proposed system are performed using phase portraits and bifurcation transition diagrams. Moreover, a design technique of a new fuzzy adaptive sliding mode control (FASMC) for synchronization of the fractional-order systems has been offered. This control technique combines an adaptive regulation scheme and a fuzzy logic controller with conventional sliding mode control for the synchronization of fractional-order systems. Applying the Lyapunov stability theorem, the proposed control technique ensures that the

master and slave chaotic systems are synchronized in the presence of dynamic uncertainties and external disturbances. The proposed control technique not only provides high performance in the presence of the dynamic uncertainties and external disturbances, but also avoids the phenomenon of chattering. Simulation results have been presented to illustrate the effectiveness of the presented control scheme.

Keywords: fractional-order four-dimensional chaotic system; self-excited and hidden attractors; multi-stability; phase portraits; bifurcation diagram; adaptive sliding mode synchronization, fuzzy adaptive sliding mode control.

1. Introduction

After the introduction of the first chaotic systems, different chaotic systems with various features including multistability [1-3], extreme multistability [4, 5], and multi-scroll attractors [6, 7] were introduced. Dynamical systems can be categorized into two general categories of dynamic systems as self-excited and hidden attractors [8, 9]. From 1994, when the first non-equilibrium chaotic flow was reported in the literature [10], almost 20 years passed before some other chaotic systems with non-equilibrium have been introduced [11-16]. It can be easily concluded that the chaotic attractor in such systems is hidden. Given that systems without equilibria have unexpected responses to perturbations, these systems have become attractive systems for researchers.

However, all the aforementioned systems with no-equilibria are described by 3D differential equations. Therefore, the research goal could be now focused on 4D dynamical systems with no-equilibria. The first 4D chaotic system was found by Rössler in 1979 [17]. In the last few years, only a few works regarding 4D chaotic dynamical systems with no-equilibria have been reported. In 2014, Wei *et al.* presented a new four-dimensional hyperchaotic system

with no-equilibria developed by extending the generalized diffusionless Lorenz equations [18]. In 2015, a no-equilibrium chaotic system with multi-wing butterfly attractors that is constructed using a state feedback controller was proposed by Tahir *et al.* [19]. Motivated by complex dynamical behaviours of chaotic systems and unusual features of hidden attractors, a novel no-equilibrium chaotic system with an exponential nonlinearity was also proposed by Pham *et al.* in 2015 [20]. Furthermore, Pham *et al.* (2016) introduced a novel four-dimensional continuous-time autonomous system with a cubic nonlinear term, which does not have equilibria [21]. In 2017, Bao *et al.* presented a memristive system, which does not display any equilibrium, but can exhibit hyperchaotic, chaotic, and periodic dynamics as well as transient hyperchaos [22]. Furthermore, in 2018, Zhang *et al.* introduced a 4D chaotic system, which was composed of nine terms including only one constant term, having also a line of equilibrium points or no equilibrium points [23].

In recent years, fractional calculus has received much attention due to fractional derivatives providing more accurate models than their integer-order counterparts and are an excellent approach to describing the memory and hereditary properties of real physical phenomena. Multiple examples can be found in different interdisciplinary fields [24], ranging from living systems (biological systems, macroeconomic models, anomalous viscoelastic diffusion in complex liquids, etc.) to non-living systems (control problems, secure communications, and so forth) [24-29]. Regarding fractional-order four-dimensional dynamical systems without equilibrium points generating hidden attractors, few works have been published. Cafagna and Grassi [30] introduced the first fractional-order 4D system without equilibrium points. That system can generate hyperchaos for proper system parameters. Volos *et al.* [31] proposed a 4-D hyperchaotic fractional-order memristive system with hidden attractors, where the type of hidden attractor belongs to a class of systems with a line of equilibria. Rajagopal *et al.* [32] reported a hyperchaotic chameleon system with fractional-order. The main characteristic of

that system was that can change between a hidden attractor without equilibrium points and self-excited attractor depending on the values of parameters. Hoang et al. [33] showed that a four-dimensional dynamical system with no-equilibrium could generate hyperchaos and coexisting chaotic attractors. Li et al. [34] proposed a new 4D fractional-order chaotic system with no equilibrium. The system can exhibit complex dynamic behaviors when its parameter and fractional derivative order are varied. Wang et al. [35] introduced a new 4D fractional-order chaotic system with hidden attractors. The abundant and complex hidden dynamical behaviors were studied by nonlinear theory, numerical simulation, and circuit realization. Also, the main mode of electrical behavior in many neuroendocrine cells, bursting oscillations (BOs) was found in that system. Zhang et al. [36] developed a novel four-dimensional fractional-order chaotic system by adding a further variable in a three-dimensional chaotic system. Also, the offset boosting of a variable was achieved by adjusting a constant term. In this manner, the research effort oriented to four-dimensional fractional-order dynamical systems with no-equilibria is vital to understand this exciting and still less-explored subject of importance.

During the past several years, various control techniques, such as: feedback control [37], adaptive control [38], fuzzy logic control [39, 40], active control [41], and sliding mode control (SMC) [42] have been proposed for synchronization of the fractional-order systems. The sliding mode approach is one of the effective robust controllers for handling complex high-order nonlinear systems [43, 44]. Hence, SMC has been repeatedly proposed for the synchronization of fractional-order chaotic systems. On the other hand, fuzzy control is one of the practical and effective methods for control of various practical uncertain systems due to its intelligent control theory [45, 46]. Therefore, many research studies have been carried out to employ fuzzy controller for nonlinear uncertain systems [47-49].

Wang et al. [50] have proposed an adaptive Takagi-Sugeno-Kang fuzzy sliding mode controller; they have used this controller for a switched reluctance motor. Muñoz-Vázquez et al. [51] have designated a model-free implementation based on the robust output feedback control for tracking of robotic manipulators. An adaptive interval type-2 fuzzy SMC has been designed by Akbarzadeh et al. [39] for synchronization of two different chaotic nonlinear systems in the presence of external disturbances and process noises. The synchronization of integer financial system with coexisting attractors has been studied using a novel fuzzy integral terminal sliding mode control by Jahanshahi et al. [52]. The control of uncertain robotic manipulators has been studied by Ravandi et al. [53]. They have integrated the fuzzy engine with SMC for an integer system in order to approximate the unknown part of the model. Polák et al. [54] have designed a fuzzy controller to combine movement detection, face detection, and the fractal dimension signals for robotic motion. Vascak et al. [55] have designated self-organizing fuzzy controller for control of aircraft. They have investigated the performance of the self-organizing fuzzy controller with some experimental results. Rajagopal et al. [56] have designed a linear quadratic regulator and a fuzzy-based PID controller for synchronization of a hyperchaotic memristor oscillator.

In the synchronization of chaotic systems, it is usually the case that some system parameters are not accurately known [57]. Besides, due to environmental conditions, the features of the system may change over time. Nevertheless, in most studies, the effects of uncertainties and disturbances have been ignored, which cannot be avoided in real systems [58]. Hence further study of the synchronization of fractional-order systems is required to achieve higher performance for these systems. Therefore, in the present study, the novel fuzzy adaptive sliding mode control (FASMC) has been proposed for synchronization of fractional-order systems. It is assumed that the plant function is not known completely. By using the Lyapunov approach, the adaptation laws are derived. The proposed control scheme is robust

against uncertainties and disturbances. Moreover, to address the chattering problem which exists in SMC, the fuzzy logic inference engine has been used. This way, chattering phenomena and convergence time of the system reduce in comparison with the conventional SMC.

This article is motivated by investigating a new multi-stable fractional-order four-dimensional system with self-excited and hidden chaotic attractors. Firstly the system's behaviour has been studied with dynamical systems analysis. Afterward, the FASMC has been proposed for synchronization of fractional-order chaotic systems. The stability and convergence of the proposed control scheme have been proved via the Lyapunov stability theorem. The conventional sliding mode control (SMC) generates chattering for uncertain systems due to the existence of discontinuous sign (s) function in the control input. The chattering causes vibration in the system. The problem of the vibration in the system has been solved by the proposed FASMC. The reasons are expressed in the following. 1) One of the significant issues in the control and synchronization of complex systems is the existence of uncertainties. In the proposed controller, we have implemented the adaption mechanism with the control scheme. The adaption mechanism estimates the parameters of the system and helps the controller to deal better with uncertainties. Hence, the vibrations in the system are decreased. 2) The fuzzy logic system has been combined with control scheme. The chattering problem is reduced by employing a fuzzy logic system; also, speed of convergence is increased. Finally, the performance of the proposed control scheme has been investigated by presenting simulation results.

2. Equilibrium points for the integer order system

The general form of the integer-order four-dimensional system is:

$$\dot{x} = y = F(x, y, z, w) \tag{1a}$$

$$\dot{y} = z = G(x, y, z, w) \quad (1b)$$

$$\dot{z} = w = H(x, y, z, w) \quad (1c)$$

$$\dot{w} = aw + bx^2 + cy^2 + exy + fxz + g = K(x, y, z, w) \quad (1d)$$

The equilibrium states are found by setting the LHS of (1) to zero. (1a)-(1c) give $y = z = w = 0$, while (1d) gives $bx^2 + g = 0$.

If b and g are both nonzero with the same signs, then there are no equilibria. If $g = 0$, then (1d) gives $x = 0$, so we have the trivial equilibrium $(0,0,0,0)$.

If b and g have opposite signs, then $x = \pm\sqrt{-g/b}$ and the system have two equilibrium points.

The linear stability of the equilibrium states is found by computing the fourth order Jacobian matrix:

$$J = \begin{pmatrix} 0 & 1 & 0 & 0 \\ 0 & 0 & 1 & 0 \\ 0 & 0 & 0 & 1 \\ 2bx + ey + fz & 2cy + ex & fx & a \end{pmatrix} \quad (2)$$

and then computing the determinant of $J - \lambda I_4$ for each equilibrium state. Here λ give the eigenvalues, and I_4 is the identity matrix.

(i) If $g = 0$, we obtain a degenerate quartic characteristic equation:

$$\lambda^4 - a\lambda^3 = 0, \quad (3)$$

so that we have a triple zero eigenvalue $\lambda = 0$, together with a fourth eigenvalue $\lambda = a$.

(ii) If $g \neq 0$, we obtain the quartic characteristic equation:

$$\lambda^4 - a\lambda^3 - fx_e\lambda^2 - ex_e\lambda - 2bx_e = 0, \quad (4)$$

where $x_e = \sqrt{-g/b}$. We now consider the possible codimension one, two and three bifurcations.

2.1. Bifurcations from the nontrivial equilibrium

When $\lambda = 0$, we have a saddle-node or a pitchfork bifurcation if $b = 0$ or $x_e = \sqrt{-g/b} = 0$. The former condition is not possible for finite equilibria, and so we require $x_e = 0$.

For a Hopf bifurcation, $\lambda = \pm\omega$ satisfies

$$\begin{aligned}\omega^4 + fx_e\omega^2 - 2bx_e &= 0, \\ a\omega^2 + ex_e &= 0\end{aligned}\tag{5}$$

The second equation gives $\omega^2 = -ex_e/a > 0$ (so that a and e must take opposite signs), while for real roots to the first equation we require $f^2x_e^2 + 8bx_e > 0$. Substituting $\omega^2 = -ex_e/a$ into the first equation gives

$$f = \frac{2ba^2 - e^2x_e}{aex_e}\tag{6}$$

A Takens-Bogdanov double-zero bifurcation occurs when $\lambda = 0$ (twice). From (4) we see that this implies that $bx_e = 0$ and $ex_e = 0$, which is satisfied by $x_e = 0$, and we recover the trivial equilibrium state. Therefore, there is no nontrivial double-zero bifurcation. The same conclusion applies to a triple-zero bifurcation.

For a Hopf-zero bifurcation, we require $x_e = 0$ for the steady bifurcation, while the Hopf bifurcation conditions yield

$$\omega^2 = ex_e/a, \omega^2 = fx_e,\tag{7}$$

but $x_e = 0$ means that $\omega = 0$, so no Hopf-zero bifurcation is possible.

2.2. Bifurcations from the nontrivial equilibrium

When the coefficient of y^2 in (1d) is negative, we find a series of period doubling cascades, as shown in Figs. 1 and 2 below. In Fig. 1, we increase g through negative values from $g = -4$ to $g = 0.75$, while in Fig. 2, we decrease g from 0.75. Hysteresis is clearly evident, especially in the range $-2 < g < 0$ and only periodic states exist when g decreases, while chaotic, periodic and period-doubled states exist when g increases. Therefore, there is evidence of multiple attractor states. Note that, since b is positive, there are no equilibria when $g > 0$, and two saddle points when $g < 0$.

Figure 3 shows phase portraits in the (x, y) -plane and $x(t)$ time series for $g = -1.0$ for the scenarios shown in Figs. 2 and 3, when the coefficient of y^2 in the equation for $\dot{\omega}$ is +0.19. Here Fig. 3(a) and (c) show a period-4 cycle when g is increasing, while in Fig. 3(b) and (d) we obtain a period-3 cycle when g is decreasing. Fig. 4 shows the corresponding plots for $g = -0.25$. Now, instead of two co-existing periodic states, we find that a chaotic attractor when g is increased coexists with a period-4 cycle when g is decreased. Fig. 5 shows a chaotic attractor for $g = 0.2$, in the region where there are no real equilibria, again when the coefficient of y^2 in the equation for $\dot{\omega}$ is +0.19.

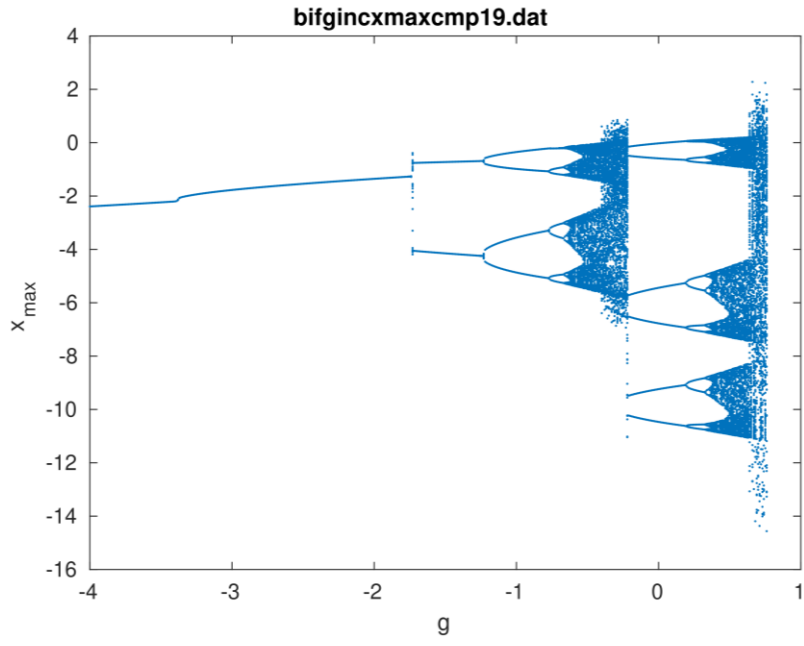


Fig. 1. A bifurcation transition diagram of x_{\max} as g increases, when $c = -0.19$, so the term in $\dot{\omega}$ is $+0.19y^2$.

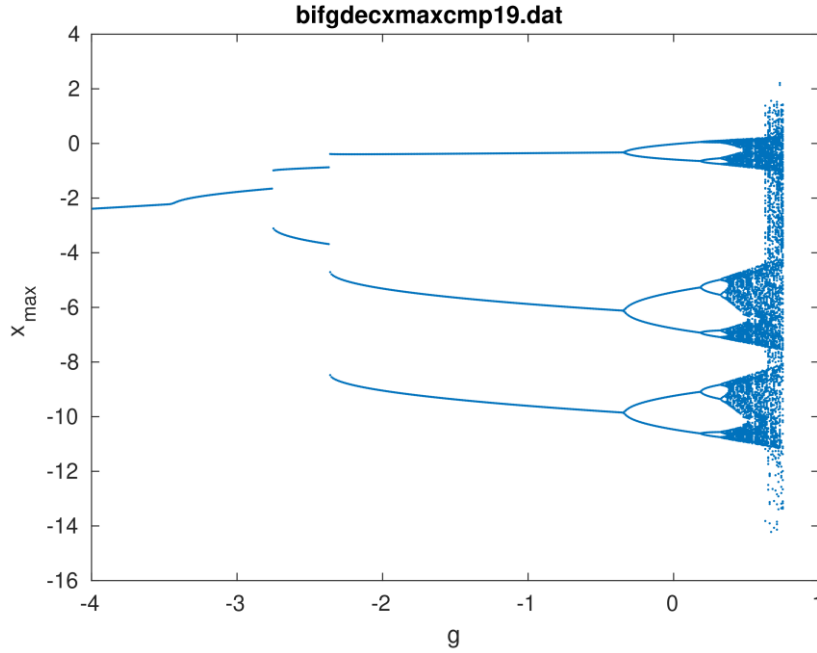


Fig. 2. A bifurcation transition diagram of x_{\max} as g decreases, when $c = -0.19$, so the term in $\dot{\omega}$ is $+0.19y^2$.

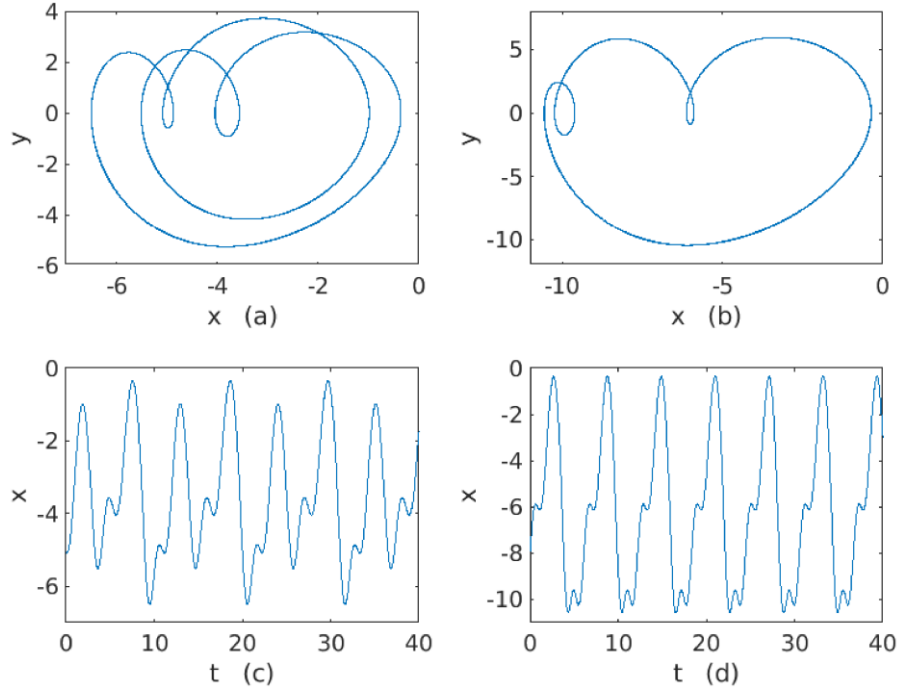


Fig. 3. Phase plots of (x, y) and time series of $x(t)$ for the given system, for $g = -1.0$ when the term in $\dot{\omega}$ is $+0.19y^2$. Here (a) and (c) are for g increasing, while (b) and (d) are for g decreasing.

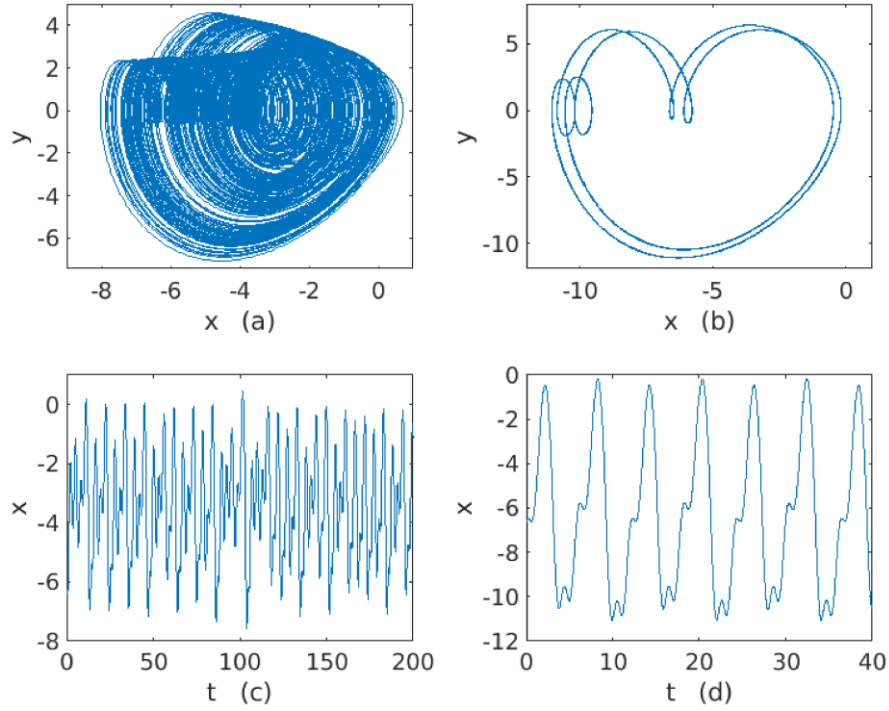


Fig. 4. Phase plots of (x, y) and time series of $x(t)$ for the given system, for $g = -0.25$ when the term in $\dot{\omega}$ is $+0.19y^2$. Here (a) and (c) are for g increasing, while (b) and (d) are for g decreasing.

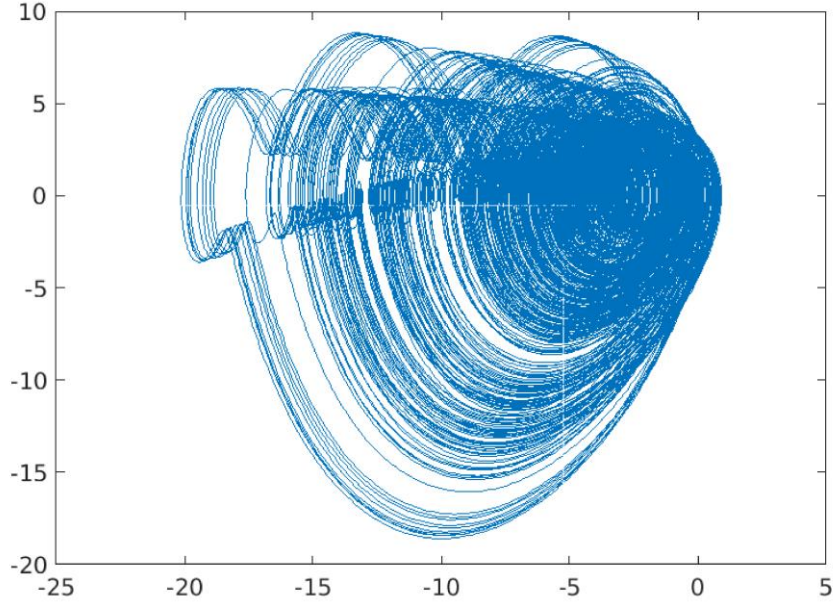


Fig. 5. Phase plot of (x, y) for the given system, when $g = 0.2$, so that there is no equilibrium state.

3. Analysis of the new fractional system

In this section, the fractional-order form of the proposed system is derived. Fractional calculus is a generalization of the differentiation and integration to non-integer order, which is expressed by the continuous integro-differential operator ${}_a D_t^q$, where a and t are the limits of the operation and $q \in \mathbb{R}$. The operator is defined as

$${}_a D_t^q = \begin{cases} \frac{d^q}{dt^q} & q > 0 \\ 1 & q = 0 \\ \int_a^t (d\tau)^q & q < 0 \end{cases} \quad (8)$$

The three most frequently used definitions for the general fractional-order operator are Riemann–Liouville (RL), Grünwald–Letnikov (GL) and Caputo (C) [59]. Focusing on the fractional derivative, the remaining question is which definition is the suitable one? Which fractional derivatives are consistent with the classic integer-order laws? Or, which fractional

derivatives are suitable for dealing with practical systems in a compatibility with integer-order definitions? [60] From a purely mathematical point of view, we could choose to use one or all the derivatives above mentioned. However, we must be suspicious since they assume underlying hypothesis that may not be verified, e.g., the RL derivative of a constant does not exist and the C derivative of the Heaviside unit step function is zero, preventing the definition of impulse response of a linear system [61]. Let us explain this. The causal Riemann-Liouville and Caputo derivatives that are currently used in most papers and books are defined by [62, 63].

$$D_{RL}^q f(t) = D^n \left\{ \frac{1}{\Gamma(\epsilon)} \int_0^t f(\tau) (t - \tau)^{\epsilon-1} d\tau \right\} \quad (9)$$

and

$$D_C^q f(t) = \frac{1}{\Gamma(-q)} \int_0^t f^{(n)}(\tau) (t - \tau)^{\epsilon-1} d\tau \quad (10)$$

The orders are given by $q = n - \epsilon$, n being the last integer greater than q and $0 < \epsilon < 1$. These definitions show that the RL and C derivatives are null for $t < 0$. The analysis given by Ortigueira [61] demonstrated that both RL derivative (9) and C derivative (10) are unable to define correctly the linear systems defined by $\sum_{k=0}^N a_k D^{q_k} y(t) = \sum_{k=0}^M b_k D^{r_k} x(t)$, where $a_N = 1$, N and M are any given positive integers, and the sequences a_k , and b_k are strictly increasing. The main reasons are *i*) the derivative of an exponential using (9) or (10) is not an exponential, *ii*) the derivative of the $\delta(t)$ is identically null when the lower limit in (9) or (10) equals 0^+ , *iii*) the derivative property of the Laplace transform $LT[D^{q_i} f(t)] = s^{q_i} F(s)$ is not valid. As a result, RL and C derivatives are less useful in signals and systems theory due to the complication about s^q [64].

3.1. Wide Sense Criterion (WSC) for fractional derivatives

In this framework, Ortigueira and Tenreiro-Machado [60, 65] proposed recently a novel criterion to determine if an operator can be classified as a Fractional Derivative or not, which is based on the criterion formulated by Ross [66]. The criterion is as follows. An operator is considered as a fractional derivative in WSC if it has the properties ²P defined as:

- a) ²P1 Linearity. The operator is linear
- b) ²P2 Identity. The zero-order derivative of a function returns the function itself.
- c) ²P3 Backward compatibility. When the order is an integer, the fractional derivative gives the same result as the ordinary derivative.
- d) ²P4 The index law holds, i.e., $D^\alpha D^\beta f(t) = D^{\alpha+\beta} f(t)$ for $\alpha < 0$ and $\beta < 0$.
- e) ²P5 Generalized Leibniz rule $D^\alpha [f(t)g(t)] = \sum_{i=0}^{\infty} \binom{\alpha}{i} D^i f(t) D^{\alpha-i} g(t)$.

Additionally, the index law property can be modified to include positive orders. This leads to the strict sense criterion (SSC).

- f) ³P4 The index law $D^\alpha D^\beta f(t) = D^{\alpha+\beta} f(t)$ for any α and β .

Under this criterion some proposed operators such as the conformable fractional derivative [67], fail some of the previous points and therefore, it cannot be considered as a fractional derivative [65].

3.2. The Grünwald–Letnikov derivative

The name “Grünwald-Letnikov derivatives” is currently adopted in derivatives based on the incremental ratio [68]. From the applied sciences point of view, the Grünwald-Letnikov fractional derivatives seem to be a natural way for generalizing the notion of derivative. They have a solid meaning for any real or complex order, and we recover the classic results for

integer-orders. The generalization of the GL fractional derivative is defined by the limit of the fractional incremental ratio [69],

$${}^{GL}D_{\theta}^q f(\zeta) = e^{-iq\theta} \lim_{|h| \rightarrow 0} \frac{\sum_{k=0}^{\infty} (-1)^k \binom{q}{k} f(\zeta - kh)}{|h|^q} \quad (11)$$

where $h = |h|e^{j\theta}$ is a complex number, and $\theta \in (-\pi, \pi]$. If $t \in \mathbb{R}$, then we could define the forward and backward derivatives. We consider the forward derivative only. When $h = |h|$ the forward GL derivative is given by

$${}^{GL}D_F^q f(t) = \lim_{|h| \rightarrow 0} \frac{\sum_{k=0}^{\infty} (-1)^k \binom{q}{k} f(t - kh)}{|h|^q} \quad (12)$$

The selection of GL derivative in this work relies on the basis that it satisfies the WSC and SSC criteria [65]. The following are the demonstrations of the criteria (see [60, 65] for details).

- The linearity is a direct characteristic of this operator.
- The additivity and commutativity can be verified by applying (12) twice for any two orders [69].

$${}^{GL}D_F^q [{}^{GL}D_F^r f(t)] = {}^{GL}D_F^r [{}^{GL}D_F^q f(t)] = {}^{GL}D_{\theta}^{q+r} f(t) \quad (13)$$

- Neutral element. When $r = -q$ in (13) and $q \rightarrow 0$ the binomial coefficients $\binom{q}{k}$ are all null excepting the first, then $f(t)$ can be recovered.

$${}^{GL}D_F^q [{}^{GL}D_F^{-q} f(t)] = {}^{GL}D_F^0 f(t) = f(t) \quad (14)$$

- Backward compatibility. By considering $q = n \in \mathbb{N}$ then,

$${}^{GL}D_F^n f(t) = \lim_{h \rightarrow 0} \frac{\sum_{k=0}^n (-1)^k \binom{n}{k} f(t - kh)}{h^n} \quad (15)$$

which is the resulting expression by the repeated application of the first-order derivative.

- Derivative of a product. The generalized Leibniz rule can be obtained by considering the product of two functions: $f(t) = \varphi(t) \cdot \psi(t)$ defined for $t \in \mathbb{R}$, under the assumption that one function is analytic in a given region.

$${}^{GL}D_F^q [\varphi(t)\psi(t)] = \sum_{n=0}^{\infty} \binom{q}{n} \varphi^{(n)}(t) {}^{GL}D_F^{q-n} \psi(t) \quad (16)$$

As a conclusion, the Grünwald-Letnikov derivative is a suitable derivative for this study.

3.3. Proposed fractional-order four-dimensional system and its numerical solution

In this manner, the integer order four-dimensional system in (1) is generalized to the fractional-order domain by applying the fractional-order operator of the forward Grünwald-Letnikov derivative in (12). Then, we obtain

$${}^{GL}D^{q_1} x = y \quad (17a)$$

$${}^{GL}D^{q_2} y = z \quad (17b)$$

$${}^{GL}D^{q_3} z = w \quad (17c)$$

$${}^{GL}D^{q_4} w = aw + bx^2 + cy^2 + exy + fxz + g \quad (17d)$$

where, (q_1, q_2, q_3, q_4) are the fractional-orders with $1 < q < 0$, and (a, b, c, e, f, g) are the system parameters. For numerical calculation of the system (19), we use the relation (12)

assuming the summation is limited to $\frac{t-\alpha}{h}$, where α is a real constant, then we can write

$${}^{GL}D_F^q f(t) = \lim_{|h| \rightarrow 0} \frac{\sum_{k=0}^{\lfloor \frac{t-\alpha}{h} \rfloor} (-1)^k \binom{q}{k} f(t-kh)}{|h|^q}, \quad (18)$$

where symbol $\lfloor \cdot \rfloor$ means the integer part of $\frac{t-\alpha}{h}$, and q , and h are the bounds of operation for ${}^{GL}D_F^q f(t)$ [59, 70]. In this manner, with some abuse of notation, the relation to the explicit numerical approximation of q -th derivative at the points lh , ($l = 1, 2, \dots$) has the following form

$$\frac{l-L_m}{h} D_{t_l}^q f(t) = h^{-q} \sum_{k=0}^l (-1)^k \binom{q}{k} f(t_{l-k}), \quad (19)$$

being L_m the memory length, $t_l = lh$, h the time step, and $(-1)^k \binom{q}{k}$ the binomial coefficients $c_k^{(q)}$. These can be calculated with $c_0^{(q)} = 1$, $c_k^{(q)} = 1 - \frac{1+q}{k} c_{k-1}^{(q)}$. Then, the numerical solution of proposed fractional-order system (17) can be expressed as

$$\begin{aligned} x(t_{k+1}) &= [y(t_k)]h^{q_1} - \sum_{k=v}^l c_k^q x(t_{l-k}), \\ y(t_{k+1}) &= [z(t_k)]h^{q_2} - \sum_{k=v}^l c_k^q y(t_{l-k}), \\ z(t_{k+1}) &= [w(t_k)]h^{q_3} - \sum_{k=v}^l c_k^q z(t_{l-k}), \\ w(t_{k+1}) &= [aw(t_k) + bx(t_k)^2 + cy(t_k)^2 + ex(t_k)y(t_k) + fx(t_k)z(t_k) + g]h^{q_4} - \\ &\quad \sum_{k=v}^l c_k^q w(t_{l-k}), \end{aligned} \quad (20)$$

where v follows the rule

$$v = \begin{cases} 1, & \text{for } l \leq \frac{L_m}{h}, \\ l - \frac{L_m}{h}, & \text{for } l > \frac{L_m}{h}. \end{cases} \quad (21)$$

L_m is the memory length which is set according to a proper accuracy.

3.4. Self-excited chaotic attractor

By considering $D^q f(x, y, z, w; t) = 0$ in system (17), if b and g have opposite signs, the

equilibrium points of the system are $E = \left(\pm \sqrt{\frac{-g}{b}}, 0, 0, 0 \right)$.

Theorem 1: Consider the following n – dimensional fractional-order system

$$\begin{aligned} D^{q_1} x_1 &= a_{11}x_1 + a_{12}x_2 + \dots + a_{1n}x_n \\ D^{q_2} x_2 &= a_{21}x_1 + a_{22}x_2 + \dots + a_{2n}x_n \\ &\vdots \\ D^{q_n} x_n &= a_{n1}x_1 + a_{n2}x_2 + \dots + a_{nn}x_n \end{aligned} \quad (22)$$

where all q_i 's are rational numbers between 0 and 1. Assume m be the lowest common

multiple of the denominators u_i 's of q_i 's, where $q_i = \frac{v_i}{u_i}$, $(u_i, v_i) = 1$, $u_i, v_i \in \mathbb{Z}^+$ for

$i = 1, 2, \dots, n$. Define

$$\Delta(\lambda) = \begin{bmatrix} \lambda^{mq_1} - a_{11} & -a_{12} & \cdots & -a_{1n} \\ -a_{21} & \lambda^{mq_2} - a_{22} & \cdots & -a_{2n} \\ \vdots & \vdots & \ddots & \vdots \\ -a_{n1} & -a_{n2} & \cdots & \lambda^{mq_n} - a_{nn} \end{bmatrix} \quad (23)$$

Then the zero solution of system (11) is globally asymptotically stable in the Lyapunov sense

if all roots λ 's of the equation $\det(\Delta(\lambda)) = 0$ satisfy $|\arg(\lambda)| > \pi/2m$. $\Delta(s)$ is called the

characteristic matrix and $\det(\Delta(\lambda))$ is called the characteristic polynomial of system (17),

[59, 71, 72].

Since the fractional-order system $D^q \psi = f(\psi)$ and the integer-order system $\dot{\psi} = f(\psi)$, with $\psi = [x, y, z, w]^T$, have the same set of equilibria in Ω , suppose Ω is the set of equilibrium points surrounded by scrolls; a necessary condition for system $D^q \psi = f(\psi)$ to exhibit a chaotic attractor is the instability of its equilibrium points in Ω [71, 72].

Case 1: Two equilibrium points $E = \left(\pm \sqrt{\frac{-g}{b}}, 0, 0, 0 \right)$

According to Theorem 1, the instability measure of the fractional-order system (17) at the equilibrium point E^* is mathematically defined by

$$\left(\frac{\pi}{2m} \right) - \min \{ |\arg(\lambda_i)| \} \geq 0, \quad (24)$$

for all roots λ_i of $\det \left(\text{diag} \left([\lambda^{mq_1} \lambda^{mq_2} \dots \lambda^{mq_n}] \right) - J \middle| E^* \right) = 0, \forall E^* \in \Omega$. By satisfying the instability measure (24), the necessary condition to observe a chaotic behavior in system (17) is obtained.

Lemma 1 When $q_1 = 0.99$, $q_2 = 0.99$, $q_3 = 0.99$, $q_4 = 0.99$, and $b = 0.7$, if $-0.55 \leq g < 0$, then system (17) exhibits a double-scroll chaotic attractor.

Proof. This proof is divided into two parts to analyze the limits of the interval for system parameter g .

- (i) The fractional-order system (17) must have the instability measure (22) with a positive sign to generate chaotic behavior. By selecting $q_1 = 0.99$, $q_2 = 0.99$, $q_3 = 0.99$, $q_4 = 0.99$, $b = 0.7$, and $g = -0.55$, equilibria are $E_1 = (0.88, 0, 0, 0)$,

$E_1 = (-0.88, 0, 0, 0)$. According to Theorem 1, the eigenvalues for equilibrium E_2 are given by:

$$\lambda^{396.00} + 1.05\lambda^{297.00} + 1.586665416\lambda^{198.00} + 1.214375207\lambda^{99.00} + 1.240967365 = 0 \quad (25)$$

with $m = 100$. It means that there are 100-sheets over Riemann surface, which contain all 396 roots [71, 72]. However, only roots in the first Riemann's sheet satisfy $-\pi/m < \varphi < \pi/m$ with $\varphi = |\arg(\lambda)|$ and therefore have a physical meaning. Roots with $|\arg(\lambda)| > \pi/m$ are not physical [71, 72]. In this case, $\lambda_{1,2} = 1.000555231 \pm 0.01381118804j$, $\varphi = 0.01380264730$ are the only roots satisfying $-0.0314 < \varphi < 0.0314$. By considering just the roots on the first Riemann's sheet, the instability measure is 0.0019. This implies that the equilibrium points E_2 are saddle points.

(ii) Similarly, when $g = -0.01$ the equilibrium points are $E_1 = (0.1195228609, 0, 0, 0)$, $E_2 = (-0.1195228609, 0, 0, 0)$. Then, the eigenvalues for E_2 are given by:

$$\lambda^{396.00} + 1.05\lambda^{297.00} + 0.2139459210\lambda^{198.00} + 0.1637463194\lambda^{99.00} + 0.1673320053 = 0 \quad (26)$$

Only the roots $\lambda_{1,2} = 0.9935992101 \pm 0.01147724509j$, $\varphi = 0.01155066806$ fulfill $-0.0314 < \varphi < 0.0314$. Hence, the instability measure is $\pi / 2m - \min(|\arg(\lambda)|) = 0.0041$.

This proof implies fractional-order (11) can exhibit a chaotic attractor when $q_1 = 0.99$, $q_2 = 0.99$, $q_3 = 0.99$, $q_4 = 0.99$, and $b = 0.7$, if $-0.55 \leq g < 0$. Figure 6 shows the self-excited chaotic attractor of the proposed fractional-order four-dimensional system by considering a commensurate fractional-order.

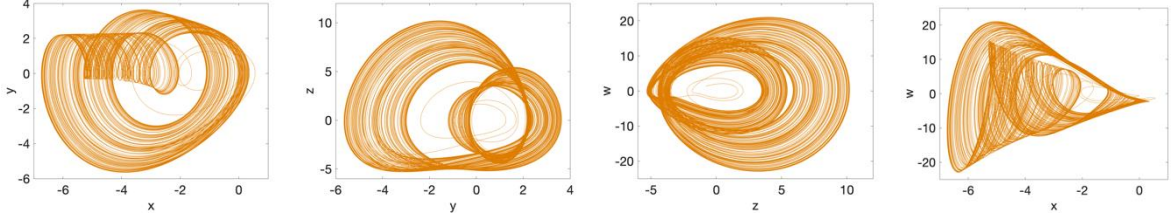


Fig. 6. 2D phase plots of the fractional-order system (17) with $q = 0.99$, $g = -0.4$, and $IC = [-4, 0.1, 0.1, 0.1]$.

To verify whether system (17) is chaotic in the classical sense, its Lyapunov exponents are calculated using the Wolf algorithm [73]. As is well known, a four-dimensional system is considered chaotic if $LE_1 > 0$, $LE_2 = 0$, $LE_{3,4} < 0$ as shown in Fig. 7 (a). Similar to the integer-order case, the parameters b, g define the stability conditions of the fractional-order four-dimensional system. When $b = 0.7$, $g = -0.4$, the system (17) generates a self-excited chaotic attractor. Figure 7(b) shows the bifurcation diagram for fractional-order q . It is observed that system (17) is driven to the mechanism of period doubling to a chaotic state. Chaos behaviour is valid from $0.98 < q \leq 1$, and therefore, the minimum effective dimension which is the sum of the fractional-orders is as low as 3.92.

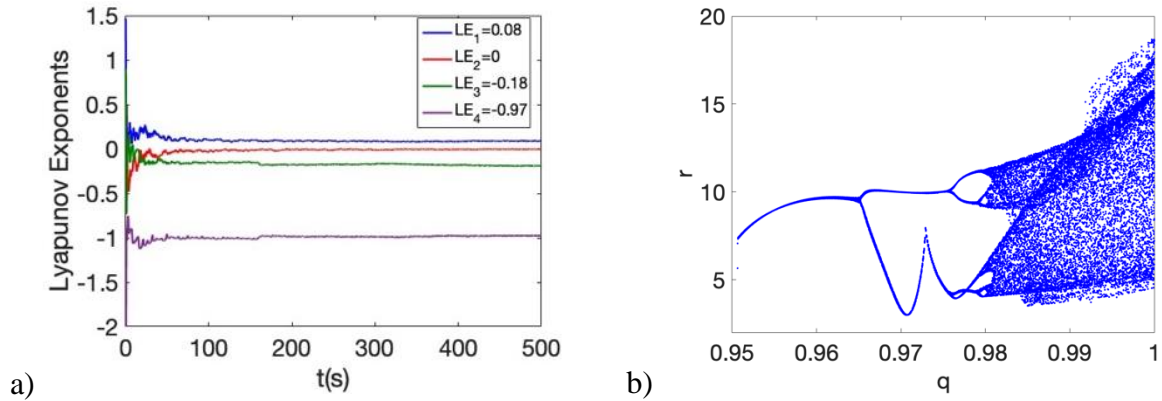


Fig. 7. a) Lyapunov exponents for the fractional-order system (17) showing a self-excited chaotic attractor. b) Bifurcation diagram for fractional-order q with $b = 0.7, g = -0.4$.

3.5. Hidden chaotic attractor without equilibrium points

Most familiar examples of chaotic flows occur in systems having one or more saddle points. However, further studies showed that there is another type of oscillations, i.e., “hidden

oscillations”. So, this class of attractors should be introduced according to the following definition:

Definition 1. *An attractor is called a self-excited attractor if its basin of attraction intersects with any open neighborhood of an equilibrium, otherwise it is called a hidden attractor [9].*

Definition 1 also includes fractional-order dynamical systems with no-equilibria, line, and surfaces of equilibria, and stable equilibria. By considering $D^q f(x, y, z, w; t) = 0$ of system (17), and b and g being both nonzero with the same signs, then there are no equilibria. As a result, the attractor generated from the system (17) is hidden and satisfies Definition 1. Figure 8 presents the hidden chaotic attractor of the fractional-order four-dimensional system (17).

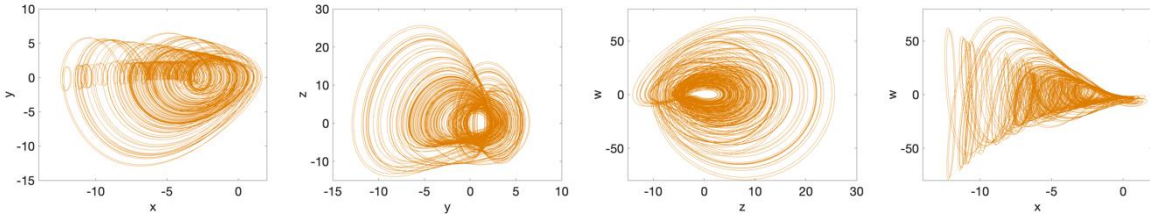


Fig. 8. 2D phase plots of the fractional-order system (17) with $q = 0.99$, $g = 0.1$, and $IC = [-10, 0.1, 0.1, 0.1]$.

Similar to the aforementioned scenario, the chaos generation is demonstrated by the Lyapunov exponents spectrum given in Fig. 9(a). The largest Lyapunov exponent LE_1 is positive indicating a chaotic behaviour. Additionally, fractional-order system (17) leads to chaotic behaviour by means of a reverse period doubling, as can be seen in the bifurcation diagram of Fig. 9(b). The hidden chaos is observed from $0.985 < q < 0.997$. Contrary to self-excited attractor case, the hidden chaos generation is only valid for fractional-orders since system (17) evolves to periodic orbits when $q = 1$.

Because the system parameter g can be defined as a control parameter for the type of chaotic attractor (hidden or self-excited), we computed a bifurcation diagram for g . Figure 10 shows the bifurcation diagram when $q = 0.99$, and $b = 0.7$. A typical mechanism of period doubling

is detected. As a conclusion, the self-excited chaotic attractor is observed for $-0.51 < g \leq 0$, whereas the hidden chaotic attractor is generated when $0 \leq g < 0.23$.

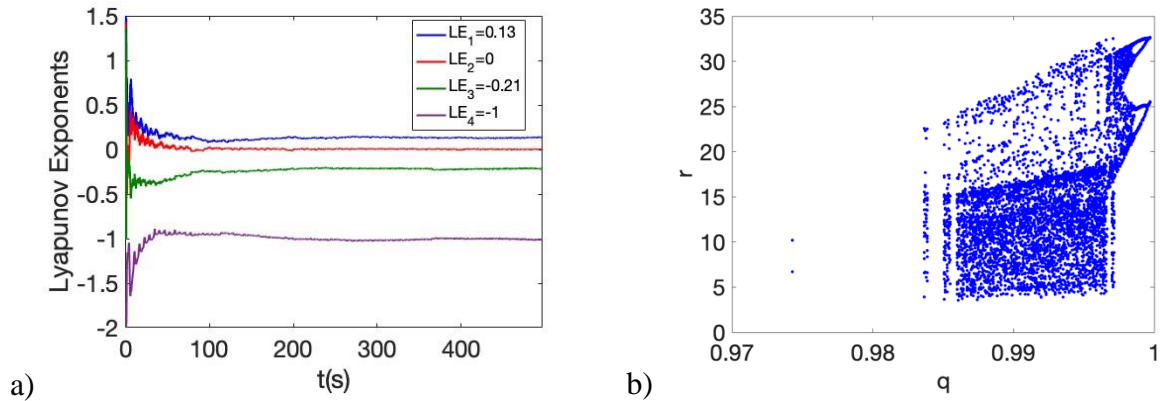


Fig. 9. a) Lyapunov exponents for the fractional-order system (17) showing a hidden chaotic attractor. b) Bifurcation diagram for fractional-order q with $b = 0.7, g = 0.1$. Finally, it is worth noting that fractional-order four-dimensional system (17) also presents the phenomenon of multi-stability which means that two or more different dynamics are generated from different initial conditions. To analyze that behaviour, we obtain bifurcation diagrams for the initial conditions as bifurcation parameters. Figure 11a, 11b, 11c, 11d, gives the bifurcation diagrams for the initial conditions $x(0), y(0), z(0), w(0)$, respectively. It is observed that system (17) evolves either unbounded orbits or hidden chaotic dynamics for distinct initial conditions $x(0), y(0), z(0)$, however, it always remains chaotic for any value of $w(0)$.

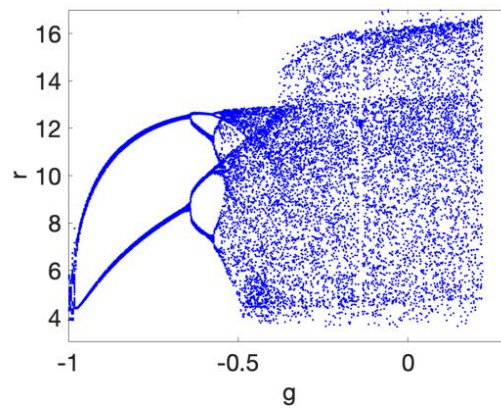


Fig. 10. Bifurcation diagram for system parameter g with $b = 0.7, q = 0.99$.

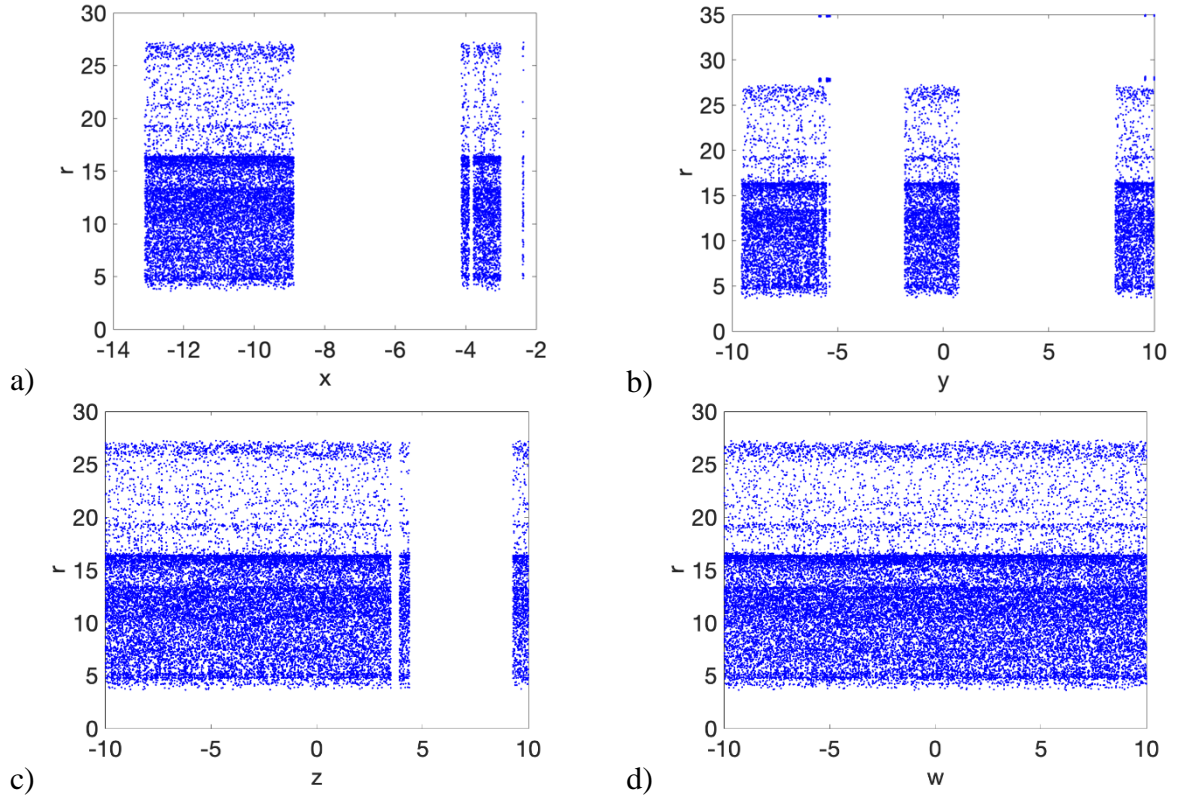


Fig. 11. Bifurcation diagrams for different initial conditions with $b = 0.7, g = 0.1, q = 0.99$, for: a) $x(0)$, b) $y(0)$, c) $z(0)$, d) $w(0)$, respectively.

The rest of this paper is devoted to the design of novel FASMC subject to the synchronization of fractional-order systems.

4. Controller design

The asymptotic stability of nonlinear fractional-order systems by using the Lyapunov method will be represented in the following:

Theorem 2 [74, 75]. Consider the fractional-order nonlinear system as

$${}_0^C D_t^\alpha x = f(t, x) \quad (27)$$

where $x=0$ is an equilibrium point for the system. Assume a positive definite function

$V(t, x(t))$ as a Lyapunov function candidate such that

$${}_0^C D_t^\beta V(t, x(t)) \leq 0 \quad (28)$$

where $\beta \in (0,1)$, then the system (27) asymptotically converges to the equilibrium point.

Lemma 2. [76] Assume that $x(t) \in \mathfrak{R}$ is a continuously differentiable function. Then, for all $t \geq t_0$ we have

$$\frac{1}{2} {}^C D_t^\alpha x^2(t) \leq x(t) {}^C D_t^\alpha x(t), \quad \forall \alpha \in (0,1) \quad (29)$$

Lemma 2 can be developed for $x(t) \in \mathfrak{R}^n$. Therefore, for $\forall t \geq t_0$ [76]

$$\frac{1}{2} {}^C D_t^\alpha x^T(t)x(t) \leq x^T(t) {}^C D_t^\alpha x(t), \quad \forall \alpha \in (0,1) \quad (30)$$

Also, Barbalat's Lemma could be developed for fractional-order systems as [77]:

Theorem 3 [77]. Consider $\phi: \mathfrak{R} \rightarrow \mathfrak{R}$ as a uniformly continuous function on the interval $[t_0, \infty)$. which ${}_0 D_t^{-\alpha} |\phi|^p \leq M$ for all $t > t_0 > 0$ where p and M are positive constants, Then

$$\lim_{t \rightarrow \infty} \phi(t) = 0 \quad (31)$$

4.1. Adaptive sliding mode synchronization

Let define the following fractional-order system with effective dimension 4α and inner dimension 4 as a slave system.

$$\begin{cases} {}^C D_t^\alpha y_1 = y_2 \\ {}^C D_t^\alpha y_2 = y_3 \\ {}^C D_t^\alpha y_3 = y_4 \\ {}^C D_t^\alpha y_4 = f(t, \mathbf{Y}) + \Delta f(t, \mathbf{Y}) + d(t) + u(t) \end{cases} \quad (32)$$

where $\mathbf{Y} = [y_1 \ \cdots \ y_n]^T$ demonstrates the system state vector. $f(t, \mathbf{Y})$ is the dynamic function. $u(t)$ and $d(t)$ denote the control input and external disturbance, respectively. In addition $\Delta f(t, \mathbf{Y}) = \mathbf{F}^T \mathbf{\Phi}$ stands for uncertain terms representing the un-modeled dynamic of the system where $\mathbf{F} = [F_1 \ F_2 \ \cdots \ F_m]^T$ is a known vector, and $\mathbf{\Phi} = [\phi_1 \ \phi_2 \ \cdots \ \phi_m]^T$

denotes the uncertain parameter vector. Now, consider the following chaotic system with fractional-order derivatives as a master system

$$\begin{cases} {}^C_0D_t^\alpha x_1 = x_2 \\ {}^C_0D_t^\alpha x_2 = x_3 \\ {}^C_0D_t^\alpha x_3 = x_4 \\ {}^C_0D_t^\alpha x_4 = h(t, \mathbf{X}) \end{cases} \quad (33)$$

where $\mathbf{X} = [x_1 \ \cdots \ x_n]^T$ denotes the measurable state vector of the master system and $h(t, \mathbf{X})$ is the nonlinear function of the master system.

In the following, the robust ASMC in fractional-order formation is employed to achieve the global synchronization between master and slave systems in the presence of uncertainties and disturbances. Difference between the states of the master and slave system is defined as the synchronization error and given by

$$e_i = x_i - y_i \quad , \quad 1 \leq i \leq 4 \quad (34)$$

considering Eqs. (32)-(34) the error dynamic can be obtained as

$$\begin{cases} {}^C_0D_t^\alpha e_1 = e_2 \\ {}^C_0D_t^\alpha e_2 = e_3 \\ {}^C_0D_t^\alpha e_3 = e_4 \\ {}^C_0D_t^\alpha e_4 = h(t, \mathbf{X}) - f(t, \mathbf{Y}) - \mathbf{F}^T \mathbf{\Phi} - d(t) - u(t) \end{cases} \quad (35)$$

where $\mathbf{\Phi}$ and $d(\cdot)$ indicate the dynamic uncertainties and disturbances as follow

$$|\phi_i| \leq \phi_i^u \quad 1 \leq i \leq 4 \quad (36)$$

$$|d(\cdot)| \leq d^u \quad (37)$$

where ϕ_i^u and d^u are constant but unknown parameters. Also, we assume that the sliding surface and all of the system state variables are continuously differentiable.

This assumption is prevalent, especially if the objective is to control a fractional-order system [78, 79]. Now, we define the sliding surface for the fractional-order system as follow

$$S = e_4 + \sum_{i=1}^4 k_i {}_0 D_t^{-\alpha} e_i \quad (38)$$

where k_1, \dots, k_4 are positive parameters. The control input is designed as

$$u = h(t, \mathbf{X}) - f(t, \mathbf{Y}) - \sum_{i=1}^m F_i \hat{\phi}_i - \hat{d} \operatorname{sgn}(S) + \mu S + \sum_{i=1}^4 k_i e_i \quad (39)$$

where $\operatorname{sgn}(\cdot)$ is the standard sign function, $\hat{\phi}_i$ and \hat{d} are adjustable parameters of the control law, which will be updated using the appropriate adaptation mechanism and μ is a positive coefficient.

Theorem 4. *By considering Eq. (39), the tracking error of the nonlinear fractional-order system (35) converges to zero based on the proposed ASMC.*

Proof. Choose Lyapunov function as

$$V(t) = \frac{1}{2} S^2 + \sum_{i=1}^m \frac{1}{2\gamma_i} (\phi_i - \hat{\phi}_i)^2 + \frac{1}{2\gamma_d} (d^u - \hat{d})^2 \quad (40)$$

the time derivative of the Lyapunov function as well as using Lemma 2 yield

$$\begin{aligned} {}^C_0 D_t^\alpha V(t) &= \frac{1}{2} {}^C_0 D_t^\alpha S^2 + \sum_{i=1}^m \left(\frac{1}{2\gamma_i} {}^C_0 D_t^\alpha (\phi_i - \hat{\phi}_i)^2 \right) + \frac{1}{2\gamma_d} {}^C_0 D_t^\alpha (d^u - \hat{d})^2 \\ &\leq S {}^C_0 D_t^\alpha S + \sum_{i=1}^m \left(\frac{1}{\gamma_i} (\phi_i - \hat{\phi}_i) {}^C_0 D_t^\alpha (\phi_i - \hat{\phi}_i) \right) + \frac{1}{\gamma_d} (d^u - \hat{d}) {}^C_0 D_t^\alpha (d^u - \hat{d}) \\ &= S \left({}^C_0 D_t^\alpha e_4 + \sum_{i=1}^4 k_i e_i \right) - \left(\sum_{i=1}^m \frac{1}{\gamma_i} (\phi_i - \hat{\phi}_i) {}^C_0 D_t^\alpha \hat{\phi}_i \right) - \frac{1}{\gamma_d} (d^u - \hat{d}) {}^C_0 D_t^\alpha \hat{d} \end{aligned} \quad (41)$$

Substituting Eq. (35) into Eq. (41) gives

$$\begin{aligned}
{}_0^c D_t^\alpha V(t) &\leq S \left(h(t, \mathbf{X}) - f(t, \mathbf{Y}) - \mathbf{F}^T \mathbf{\Phi} - d(t) - u(t) + \sum_{i=1}^4 k_i e_i \right) \\
&\quad - \sum_{i=1}^m \frac{1}{\gamma_i} (\phi_i - \hat{\phi}_i) {}_0^c D_t^\alpha \hat{\phi}_i - \frac{1}{\gamma_d} (d^u - \hat{d}) {}_0^c D_t^\alpha \hat{d}
\end{aligned} \tag{42}$$

Considering Eqs. (39) and (42), results in:

$$\begin{aligned}
{}_0^c D_t^\alpha V(t) &\leq S \left(h(t, \mathbf{X}) - f(t, \mathbf{Y}) - \mathbf{F}^T \mathbf{\Phi} - d(t) + \sum_{i=1}^4 k_i e_i \right) \\
&\quad - S \left(h(t, \mathbf{X}) - f(t, \mathbf{Y}) - \sum_{i=1}^m F_i \hat{\phi}_i - \hat{d} \operatorname{sgn}(S) + \mu S + \sum_{i=1}^4 k_i e_i \right) \\
&\quad - \sum_{i=1}^m \frac{1}{\gamma_i} (\phi_i - \hat{\phi}_i) {}_0^c D_t^\alpha \hat{\phi}_i - \frac{1}{\gamma_d} (d^u - \hat{d}) {}_0^c D_t^\alpha \hat{d} \\
&\leq |S| (d^u - \hat{d}) + S \left(\sum_{i=1}^m F_i (\phi_i - \hat{\phi}_i) \right) - \sum_{i=1}^m \frac{1}{\gamma_i} (\phi_i - \hat{\phi}_i) {}_0^c D_t^\alpha \hat{\phi}_i - \frac{1}{\gamma_d} (d^u - \hat{d}) {}_0^c D_t^\alpha \hat{d} - \mu S^2.
\end{aligned} \tag{43}$$

According to Eq. (43), to prove the stability of the closed-loop system, the adaptation laws should be considered as follows:

$${}_0^c D_t^\alpha \hat{\phi}_i = \gamma_i S F_i \tag{44}$$

$${}_0^c D_t^\alpha \hat{d} = \gamma_d |S|. \tag{45}$$

Substituting adaptation laws (44) and (45) into Eq. (43), we obtain

$${}_0^c D_t^\alpha V(t) \leq -\mu S^2. \tag{46}$$

Integrating both sides of Eq. (46) yields

$$\begin{aligned}
{}_0 D_t^{-\alpha} {}_0^c D_t^\alpha V &= V(t) - V(0) \leq -{}_0 D_t^{-\alpha} (\mu S^2) = -\mu {}_0 D_t^{-\alpha} (|S|^2) \Rightarrow \\
V(t) + \mu {}_0 D_t^{-\alpha} (|S|^2) &\leq V(0).
\end{aligned} \tag{47}$$

Since the function $V(t)$ is positive definite, one obtains

$$\mu {}_0D_t^{-\alpha}(|S|^2) \leq V(0) \Rightarrow {}_0D_t^{-\alpha}(|S|^2) \leq \frac{V(0)}{\mu}. \quad (48)$$

According to Theorem 2, Theorem 3, Eqs. (46) and (48), it is clear that the sliding surface asymptotically converges to zero, and due to asymptotic stability of the origin in the sliding surface, the synchronization error converges to zero. Therefore, the proposed control law guarantees the synchronization between master and slave systems in the presence of dynamic uncertainty and extremal disturbances. Consequently, this finishes the proof.

Remark 1. Based on theorem 4, the stability of the closed-loop system has been guaranteed via the Lyapunov stability theorem in the presence of uncertainties and disturbances which proves that the proposed control is robust against uncertainties and disturbances.

Remark 2. In the proposed controller, the adaption mechanism will estimate the parameters of the system and help the controller to better deal with the uncertain condition. Hence, the vibrations in the response of the system will be decreased [80].

4.2. Fuzzy logic

The main problems of the SMC are the existence of chattering due to the discontinuous function $\text{sgn}(\cdot)$. To address this problem, a fuzzy logic controller is proposed here. Moreover, using fuzzy logic, the gain μ_f is tuned according to the distance of the system to the sliding surface and its derivative. This way, the control effort, and tracking error are reduced. By employing the fuzzy controller the overall control law is given by

$$u = h(t, \mathbf{X}) - f(t, \mathbf{Y}) - \sum_{i=1}^m F_i \hat{\phi}_i - \hat{d}F_s + \mu_f S + \sum_{i=1}^4 k_i e_i \quad (49)$$

The fuzzy rules have been employed to obtain variables F_s and μ_f based on the variables S and S_d , where S_d is ${}_0^C D_t^\alpha S$. The fuzzy rules of the proposed controller are selected somehow

satisfy the stability of the closed-loop system. Therefore, due to stability conditions of the proposed ASMC, positiveness or negativeness of F_s is taken from variable S .

Mamdani's minimum operator with the centroid defuzzification method has been used for fuzzy implication. Max operator is used for the aggregation of the rules. Also, Min operator is used for the conjunction operator and the t-norm from the compositional rule. Figs. 12 and 13 show the Gaussian membership function of input and output linguistic variables, respectively.

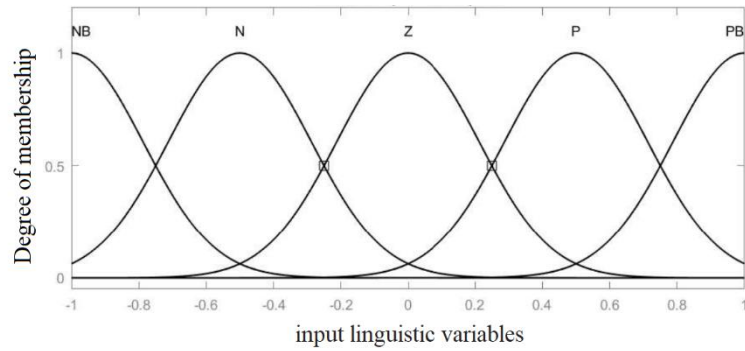


Fig. 12. Membership functions of input linguistic variables S and \dot{S} .

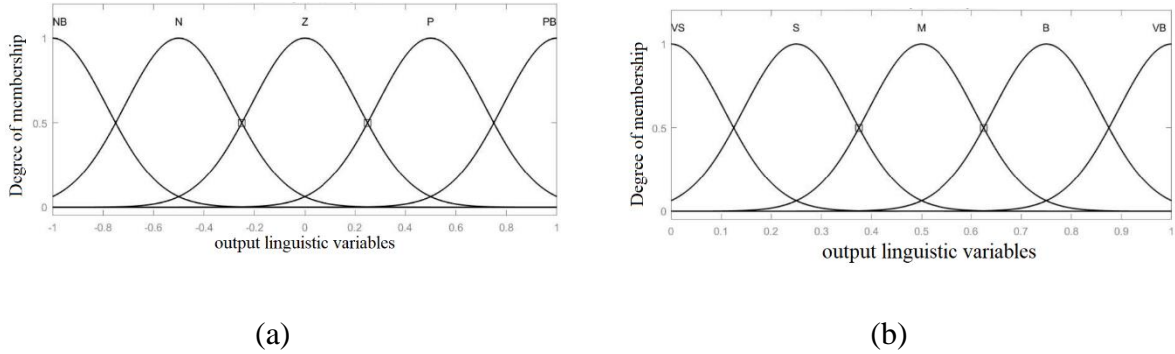


Fig. 13. Membership functions of (a) output linguistic variable F_s (b) output linguistic variable μ_f .

The membership functions for variables S , S_d and F_s have been considered as five fuzzy partitions where the following symbols have been used: PB (Positive Big), P (Positive), Z (Zero), N (Negative) and NB (Negative Big) and the fuzzy set is normalized in the interval (-

1,1). Also, for positive variable μ_f , the membership functions have been introduced as VB (very big), B (big), M (medium), S (small) and VS (very small), and the normalized interval is (0,1). Tables 1 and 2 introduce the fuzzy rules which have been implemented in the present study. The fuzzy rules which have been implemented in the present study have been introduced in Tables 1 and 2.

Table 1. Fuzzy rule of the learning rate variable F_s .

	S_d					
		NB	N	Z	P	PB
S	NB	NB	NB	N	NB	NB
	N	NB	N	N	N	NB
	Z	N	N	Z	P	P
	P	PB	P	P	P	PB
	PB	PB	PB	P	PB	PB

Table 2. Fuzzy rule of the learning rate variable μ_f .

	S_d					
		NB	N	Z	P	PB
S	NB	VB	VB	B	VB	VB
	N	B	B	M	B	B
	Z	M	M	M	M	M
	P	B	B	M	B	B
	PB	VB	VB	B	VB	PB

The procedure of FASMC for the fractional-order system is illustrated in Fig. 14. The fuzzy logic inference engine and adaptation mechanism have been combined with conventional SMC to improve the performance of the controller in the presence of dynamic uncertainties and external disturbances.

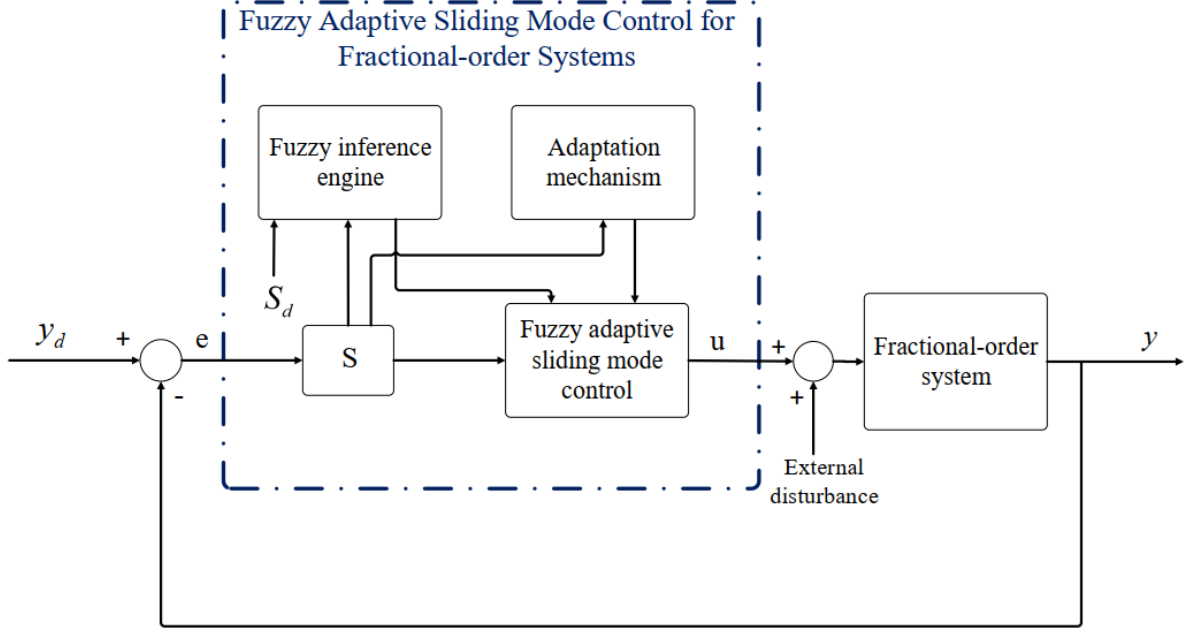


Fig. 14. Scheme of FASMC for fractional-order systems.

In the proposed FASMC, instead of the discontinuous function $\text{sgn}(\cdot)$, the fuzzy engine is employed to reduce the chattering phenomena and achieve the continuously smooth control input. In order to annihilate the chattering from the system, some research studies propose to use a saturation function $\text{sat}(\frac{s}{\Phi})$ instead of $\text{sgn}(\cdot)$ [81]. The saturation function is defined as

$$\text{sat}(s, \Phi) = \begin{cases} \text{sgn}(s) & \text{if } |s| > \Phi \\ \frac{s}{\Phi} & \text{if } |s| \leq \Phi \end{cases} \quad (50)$$

where the parameter Φ is the boundary layer thickness which is defined around the sliding surface $s = 0$. However, this solution may add a steady-state error into the sliding manifold [82]. Although the boundary layer method is used to avoid the chattering phenomena, there exists a tradeoff between the control smoothness and tracking error. To overcome this issue, in this study, the fuzzy logic system has been proposed to reduce\eliminate the chattering without sacrificing the tracking accuracy.

Moreover, in the proposed FASMC, the gain μ_f is tuned according to the distance of the system to the sliding surface and its derivative. In the uncertain condition when this gain is

tuned by the fuzzy engine as a result, tracking error will be reduced, and the speed of convergence to the desired path will be increased in comparison with conventional SMC. Therefore, the sliding surface converges to zero faster. It should be mentioned that in comparison with conventional SMC, the proposed method is more complicated and needs to implement a fuzzy engine for practical application.

4.3. Simulation results

In this section, synchronization results of uncertain fractional-order four-dimensional system in the presence of external disturbance have been presented. The governing equation of the master system is considered as follow:

$$\begin{cases} {}^C_0D_t^\alpha x_1 = x_2 \\ {}^C_0D_t^\alpha x_2 = x_3 \\ {}^C_0D_t^\alpha x_3 = x_4 \\ {}^C_0D_t^\alpha x_4 = ax_4 + bx_1^2 + cx_2^2 + ex_1x_2 + fx_1x_3 + p \end{cases} \quad (51)$$

where the parameters of the system are $\alpha = 0.97$, $a = -1.05$, $b = 0.7$, $c = -0.19$, $e = 1.37$, $f = 1.79$, and $p = -0.2$. The initial conditions for the master system are $X_0 = [0 \quad -1 \quad 0 \quad -1.5]^T$. The PECE algorithm [83] is used to solve the fractional differential equation of the system. The governing equation of the slave system can be described by the following equation:

$$\begin{cases} {}^C_0D_t^{0.97} y_1 = y_2 \\ {}^C_0D_t^{0.97} y_2 = y_3 \\ {}^C_0D_t^{0.97} y_3 = y_4 \\ {}^C_0D_t^{0.97} y_4 = \phi_1 y_4 + \phi_2 y_1^2 + \phi_3 y_2^2 + \phi_4 y_1 y_2 + \phi_5 y_1 y_3 + p + d(t) + u(t) \end{cases} \quad (52)$$

In this case, $d(t)$ is considered as $0.2\sin(t)+0.1\cos(t)$. Also, we consider $f(t, \mathbf{Y}) = p = -0.2$ and according to the proposed control technique \mathbf{F} and $\mathbf{\Phi}$ are described as:

$$\mathbf{F} = \begin{bmatrix} y_4 & y_1^2 & y_2^2 & y_1 y_2 & y_1 y_3 \end{bmatrix}^T \quad (53)$$

$$\mathbf{\Phi} = \begin{bmatrix} \phi_1 & \phi_2 & \phi_3 & \phi_4 & \phi_5 \end{bmatrix}^T \quad (54)$$

For this case study, the adaptation coefficients are chosen as $\gamma_d = 1$ and $\gamma = [0.5 \ 0.5 \ 0.5 \ 0.5]^T$. Also, in the FASMC, the parameter μ_f has been obtained by the fuzzy engine, and in ASMC we have considered $\mu = 2.5$. The initial conditions are $\mathbf{Y}(0) = [1 \ 1 \ 1 \ 1 \ 1]^T$, $\hat{\mathbf{\Phi}}(0) = [1 \ 1 \ 1 \ 1 \ 1]^T$, $\hat{k}(0) = 0.1$.

The simulation results of the adaptive synchronization are illustrated in Figs. 15-18. Tracking states of the master system via the slave system by applying ASMC and FASMC are illustrated in Figure 15. After less than 15 time units, synchronization is completely achieved, and the slave system is following the master system. Fig. 16, shows the time history of the synchronization errors. From fig 16 it can be concluded that the synchronization errors have been suppressed after a short period of time. Also, as illustrated in this figure, the system with FASMC has a smooth and chattering-free response, due to the proposed fuzzy inference engine.

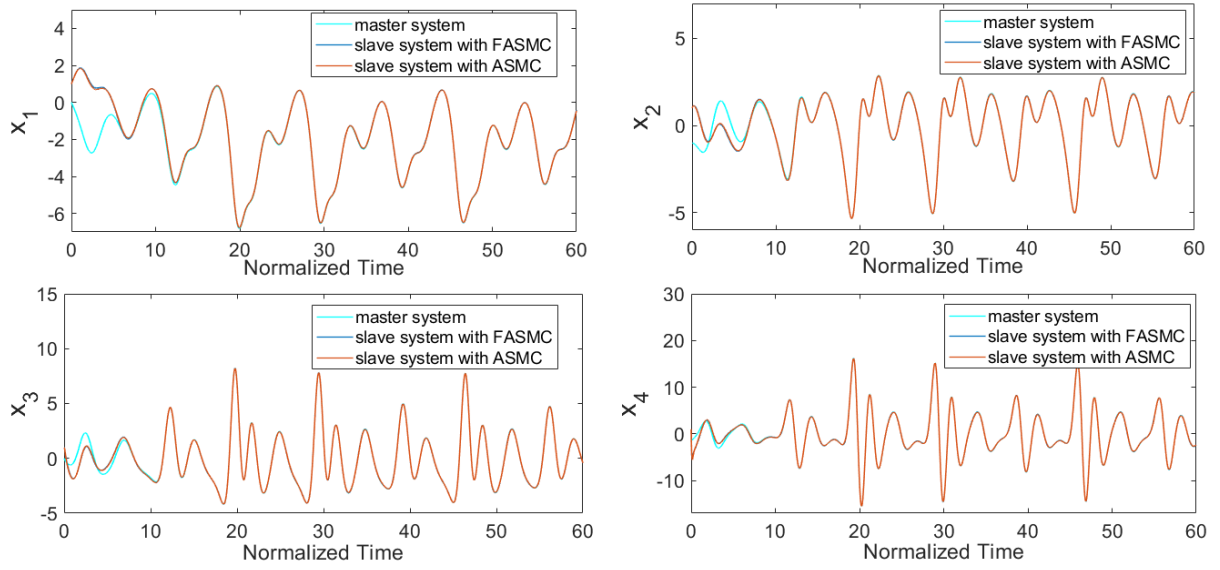


Fig. 15. Synchronization results for the fractional-order four-dimensional system with the FASMC and ASMC.

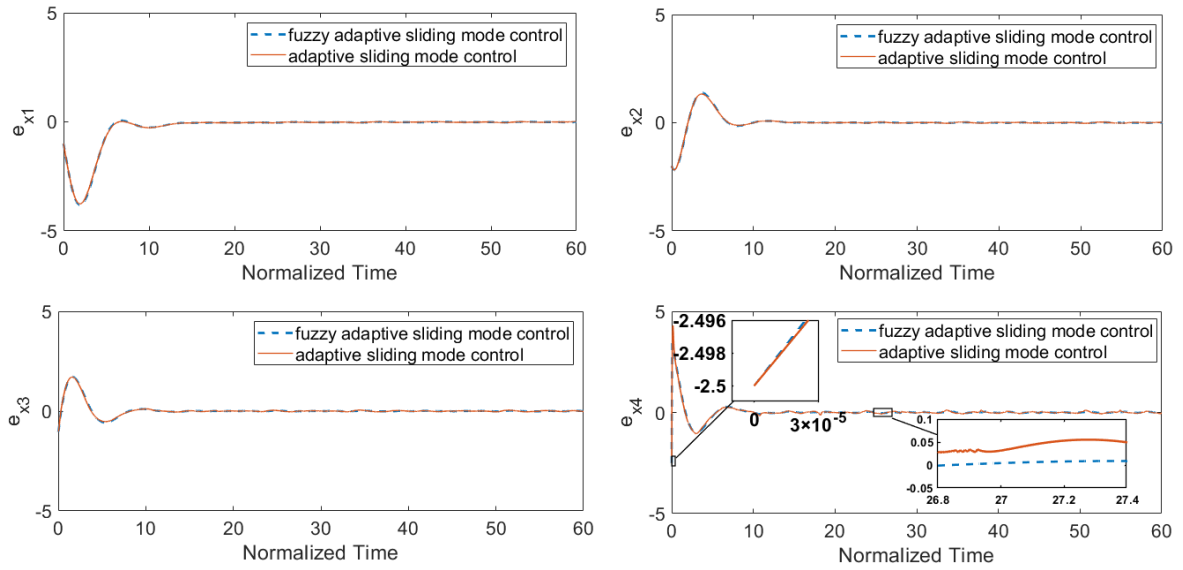


Fig. 16. Synchronization error of the fractional-order four-dimensional system with the FASMC and ASMC.

The time history of the control input and sliding surface by applying both controllers are illustrated in and Fig. 17 and 18 respectively. As observed, the sliding surface converges to zero using both FASMC and ASMC. Also, by comparing the results of FASMC and ASMC, we found that the fuzzy inference engine improves the performance of the control scheme

significantly. It is worthy to note that, maybe we could design parameter μ for ASMC in the ideal condition (without the existence of unknown disturbances and uncertainties) to achieve response similar to FASMC. But if we set the control parameter for one situation maybe these parameters don't work appropriately for another uncertain situation. Actually, this dependence is a defect for complex dynamic systems. To solve this problem a fuzzy controller is designed. It is obvious, when the system is in the presence of unknown disturbances and uncertainties the fuzzy engine by tuning the parameter μ_f will significantly improve the performance of the system.

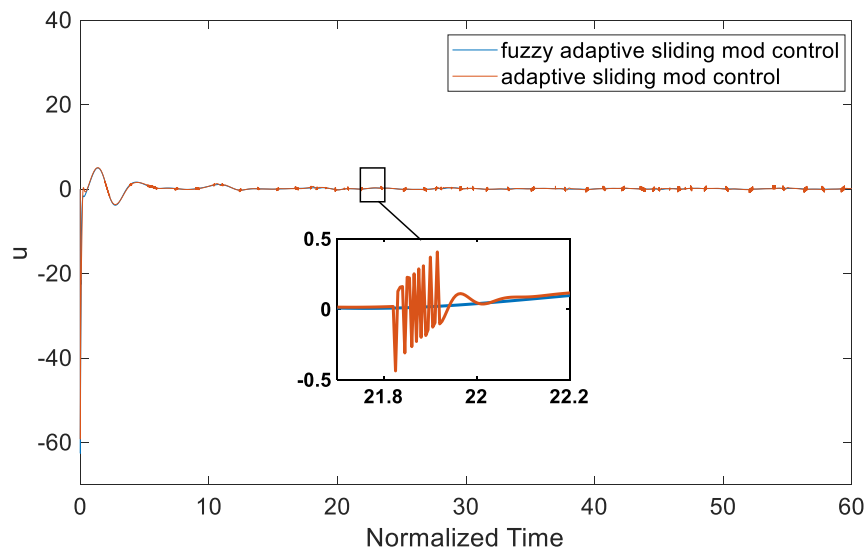


Fig. 17. The control input for synchronization of the fractional-order four-dimensional system with the FASMC and ASMC.

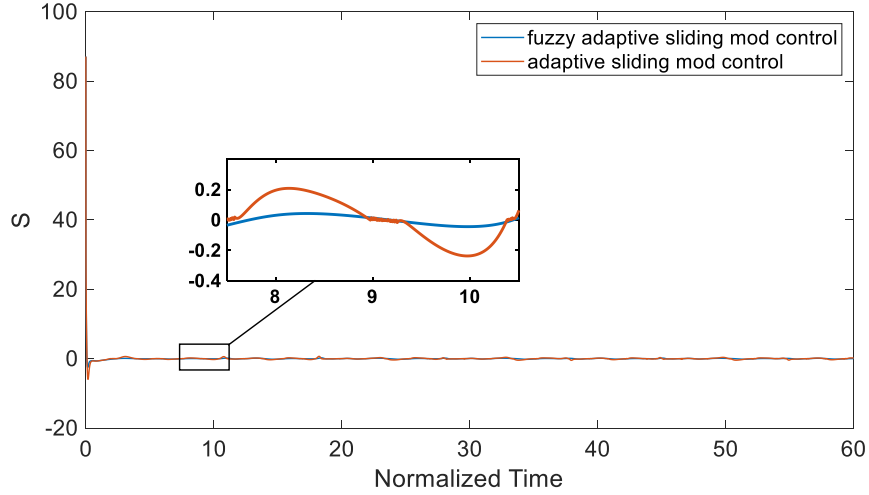


Fig. 18. Time history of sliding surface for synchronization of the fractional-order four-dimensional system with the FASMC and ASMC.

Table 1: The norms of synchronization errors and control input

	$\ u\ _2$	$\ e_{x1}\ _2$	$\ e_{x2}\ _2$	$\ e_{x3}\ _2$	$\ e_{x4}\ _2$
FASMC	161.8006	41.3710	20.2023	16.8297	21.2035
ASMC	183.6962	46.0478	27.1329	17.2352	26.0717

The values of the control input and synchronization errors based on both designed controllers are presented in tables 1. Symbol $\| \cdot \|_2$ indicates Euclidian norm. The value of synchronization errors and control input using FASMC are smaller than ASMC. the major problem in ASMC is chattering. Actually, chattering and vibration in the control input cause larger control input as well as larger synchronization errors.

Conclusion

This paper presented a novel 4D fractional-order chaotic system with specific features. Dynamic behaviours of the system were discovered by bifurcation, phase portraits, and Lyapunov exponents diagrams. Moreover, using the Lyapunov approach, the novel FASMC was designed for synchronization of the fractional-order system in the presence of uncertainties and external disturbances. From simulation results, it can be concluded that the

using designed controller, the synchronization errors have been suppressed after a short period of time. Also, the chattering problem in ASMC has been resolved by applying a fuzzy logic inference engine. In the next works, we will investigate the practical applications of the proposed system. For example, because of system's chaotic dynamics, this system is useful for developing chaos-based applications. Also, as a future suggestion, in order to mitigate the unnecessary waste of computation and communication resources the proposed control scheme could be extended by event trigger approach. In this way, the control input as a discrete-time signal could operate in an aperiodic time-triggered manner based on the event trigger strategy.

Acknowledgements

Jesus M. Munoz-Pacheco was supported by CONACYT/Mexico, Proyecto Apoyado por el Fondo Sectorial de Investigacion para la Educacion [No.258880].

Zhouchao Wei is supported by the National Natural Science Foundation of China (11772306), Graduates education Teaching Research and Reform Project of China University of Geosciences (YJS2018311), and the Fundamental Research Funds for the Central Universities, China University of Geosciences (CUGGC05).

References

- [1] Sharma PR, Shrimali MD, Prasad A, Kuznetsov NV, Leonov GA. Control of multistability in hidden attractors. *The European Physical Journal Special Topics*. 2015;224:1485-91.
- [2] Lai Q, Chen S. Generating multiple chaotic attractors from Sprott B system. *International Journal of Bifurcation and Chaos*. 2016;26:1650177.
- [3] Sprott JC, Jafari S, Khalaf AJM, Kapitaniak T. Megastability: Coexistence of a countable infinity of nested attractors in a periodically-forced oscillator with spatially-periodic damping. *The European Physical Journal Special Topics*. 2017;226:1979-85.
- [4] Bao B-C, Xu Q, Bao H, Chen M. Extreme multistability in a memristive circuit. *Electronics Letters*. 2016;52:1008-10.
- [5] Bao B, Jiang T, Xu Q, Chen M, Wu H, Hu Y. Coexisting infinitely many attractors in active band-pass filter-based memristive circuit. *Nonlinear Dynamics*. 2016;86:1711-23.

- [6] Tlelo-Cuautle E, Rangel-Magdaleno JJ, Pano-Azucena AD, Obeso-Rodelo PJ, Nuñez-Perez JC. FPGA realization of multi-scroll chaotic oscillators. *Communications in Nonlinear Science and Numerical Simulation*. 2015;27:66-80.
- [7] Munoz-Pacheco JM, Tlelo-Cuautle E, Toxqui-Toxqui I, Sanchez-Lopez C, Trejo-Guerra R. Frequency limitations in generating multi-scroll chaotic attractors using CFOAs. *International Journal of Electronics*. 2014;101:1559-69.
- [8] Wei Z, Moroz I, Sprott JC, Akgul A, Zhang W. Hidden hyperchaos and electronic circuit application in a 5D self-exciting homopolar disc dynamo. *Chaos: An Interdisciplinary Journal of Nonlinear Science*. 2017;27:033101.
- [9] Leonov GA, Kuznetsov NV. Hidden attractors in dynamical systems. From hidden oscillations in Hilbert–Kolmogorov, Aizerman, and Kalman problems to hidden chaotic attractor in Chua circuits. *International Journal of Bifurcation and Chaos*. 2013;23:1330002.
- [10] Sprott JC. Some simple chaotic flows. *Physical review E*. 1994;50:R647.
- [11] Pham V-T, Volos C, Jafari S, Kapitaniak T. Coexistence of hidden chaotic attractors in a novel no-equilibrium system. *Nonlinear Dynamics*. 2017;87:2001-10.
- [12] Pham V-T, Jafari S, Volos C, Gotthans T, Wang X, Hoang DV. A chaotic system with rounded square equilibrium and with no-equilibrium. *Optik-International Journal for Light and Electron Optics*. 2017;130:365-71.
- [13] Jafari S, Sprott JC, Golpayegani SMRH. Elementary quadratic chaotic flows with no equilibria. *Physics Letters A*. 2013;377:699-702.
- [14] Wei Z. Dynamical behaviors of a chaotic system with no equilibria. *Physics Letters A*. 2011;376:102-8.
- [15] Pham V-T, Akgul A, Volos C, Jafari S, Kapitaniak T. Dynamics and circuit realization of a no-equilibrium chaotic system with a boostable variable. *AEU-International Journal of Electronics and Communications*. 2017;78:134-40.
- [16] Ren S, Panahi S, Rajagopal K, Akgul A, Pham V-T, Jafari S. A new chaotic flow with hidden attractor: the first hyperjerk system with no equilibrium. *Zeitschrift für Naturforschung A*. 2018;73:239-49.
- [17] Rossler OE. An equation for hyperchaos. *Physics Letters A*. 1979;71:155-7.
- [18] Wei Z, Wang R, Liu A. A new finding of the existence of hidden hyperchaotic attractors with no equilibria. *Mathematics and Computers in Simulation*. 2014;100:13-23.
- [19] Tahir FR, Jafari S, Pham V-T, Volos C, Wang X. A novel no-equilibrium chaotic system with multiwing butterfly attractors. *International Journal of Bifurcation and Chaos*. 2015;25:1550056.
- [20] Pham VT, Vaidyanathan S, Volos CK, Jafari S. Hidden attractors in a chaotic system with an exponential nonlinear term. *The European Physical Journal Special Topics*. 2015;224:1507-17.
- [21] Pham V-T, Vaidyanathan S, Volos C, Jafari S, Kingni ST. A no-equilibrium hyperchaotic system with a cubic nonlinear term. *Optik-International Journal for Light and Electron Optics*. 2016;127:3259-65.
- [22] Bao BC, Bao H, Wang N, Chen M, Xu Q. Hidden extreme multistability in memristive hyperchaotic system. *Chaos, Solitons & Fractals*. 2017;94:102-11.
- [23] Zhang S, Zeng Y, Li Z, Wang M, Xiong L. Generating one to four-wing hidden attractors in a novel 4D no-equilibrium chaotic system with extreme multistability. *Chaos: An Interdisciplinary Journal of Nonlinear Science*. 2018;28:013113.
- [24] Sun H, Zhang Y, Baleanu D, Chen W, Chen Y. A new collection of real world applications of fractional calculus in science and engineering. *Communications in Nonlinear Science and Numerical Simulation*. 2018.
- [25] Wu X, Wang H, Lu H. Modified generalized projective synchronization of a new fractional-order hyperchaotic system and its application to secure communication. *Nonlinear Analysis: Real World Applications*. 2012;13:1441-50.
- [26] Hamamci SE. An algorithm for stabilization of fractional-order time delay systems using fractional-order PID controllers. *IEEE transactions on automatic control*. 2007;52:1964-9.

- [27] Zambrano-Serrano E, Muñoz-Pacheco JM, Gómez-Pavón LC, Luis-Ramos A, Chen G. Synchronization in a fractional-order model of pancreatic β -cells. *The European Physical Journal Special Topics*. 2018;227:907-19.
- [28] Alkahtani B, Atangana A. Chaos on the Vallis model for El Niño with fractional operators. *Entropy*. 2016;18:100.
- [29] Chen W-C. Nonlinear dynamics and chaos in a fractional-order financial system. *Chaos, Solitons & Fractals*. 2008;36:1305-14.
- [30] Cafagna D, Grassi G. Fractional-order systems without equilibria: the first example of hyperchaos and its application to synchronization. *Chinese Physics B*. 2015;24:080502.
- [31] Volos C, Pham VT, Zambrano-Serrano E, Munoz-Pacheco JM, Vaidyanathan S, Tlelo-Cuautle E. Analysis of a 4-D hyperchaotic fractional-order memristive system with hidden attractors. *Advances in Memristors, Memristive Devices and Systems*: Springer; 2017. p. 207-35.
- [32] Rajagopal K, Karthikeyan A, Duraisamy P. Hyperchaotic chameleon: fractional order FPGA implementation. *Complexity*. 2017;2017.
- [33] Vo Hoang D, Takougang Kingni S, Pham V-T. A no-equilibrium hyperchaotic system and its fractional-order form. *Mathematical Problems in Engineering*. 2017;2017.
- [34] Li X, Li Z. Hidden extreme multistability generated from a fractional-order chaotic system. *Indian Journal of Physics*. 2019;1-10.
- [35] Wang MJ, Liao XH, Deng Y, Li ZJ, Zeng YC, Ma ML. Bursting, Dynamics, and Circuit Implementation of a New Fractional-Order Chaotic System With Coexisting Hidden Attractors. *Journal of Computational and Nonlinear Dynamics*. 2019;14:071002.
- [36] Zhang X, Li Z. Hidden extreme multistability in a novel 4D fractional-order chaotic system. *International Journal of Non-Linear Mechanics*. 2019;111:14-27.
- [37] Zouari F, Boulkroune A, Ibeas A. Neural adaptive quantized output-feedback control-based synchronization of uncertain time-delay incommensurate fractional-order chaotic systems with input nonlinearities. *Neurocomputing*. 2017;237:200-25.
- [38] Yousefpour A, Jahanshahi H, Munoz-Pacheco JM, Bekiros S, Wei Z. A fractional-order hyperchaotic economic system with transient chaos. *Chaos, Solitons & Fractals*. 2020;130:109400.
- [39] Akbarzadeh-T MR, Hosseini SA, Naghibi-Sistani MB. Stable indirect adaptive interval type-2 fuzzy sliding-based control and synchronization of two different chaotic systems. *Applied Soft Computing*. 2017;55:576-87.
- [40] Mohammadzadeh A, Ghaemi S, Kaynak O, Khanmohammadi S. Observer-based method for synchronization of uncertain fractional order chaotic systems by the use of a general type-2 fuzzy system. *Applied Soft Computing*. 2016;49:544-60.
- [41] Bhalekar S, Daftardar-Gejji V. Synchronization of different fractional order chaotic systems using active control. *Communications in Nonlinear Science and Numerical Simulation*. 2010;15:3536-46.
- [42] Hosseinnia SH, Ghaderi R, Mahmoudian M, Momani S. Sliding mode synchronization of an uncertain fractional order chaotic system. *Computers & Mathematics with Applications*. 2010;59:1637-43.
- [43] Jahanshahi H. Smooth control of HIV/AIDS infection using a robust adaptive scheme with decoupled sliding mode supervision. *The European Physical Journal Special Topics*. 2018;227:707-18.
- [44] Amirkhani S, Mobayen S, Iliaee N, Boubaker O, Hosseinnia SH. Fast terminal sliding mode tracking control of nonlinear uncertain mass-spring system with experimental verifications. *International Journal of Advanced Robotic Systems*. 2019;16:1729881419828176.
- [45] Castillo O, Melin P. A review on the design and optimization of interval type-2 fuzzy controllers. *Applied Soft Computing*. 2012;12:1267-78.
- [46] Castillo O, Aguilar LT. Fuzzy Lyapunov Synthesis for Nonsmooth Mechanical Systems. *Type-2 Fuzzy Logic in Control of Nonsmooth Systems*: Springer; 2019. p. 43-54.
- [47] Castillo O. Framework for Optimization of Intuitionistic and Type-2 Fuzzy Systems in Control Applications. *Recent Advances in Intuitionistic Fuzzy Logic Systems*: Springer; 2019. p. 79-86.

- [48] Cheng K-H. Adaptive B-spline-based fuzzy sliding-mode control for an auto-warehousing crane system. *Applied Soft Computing*. 2016;48:476-90.
- [49] Martínez R, Castillo O, Aguilar LT. Optimization of interval type-2 fuzzy logic controllers for a perturbed autonomous wheeled mobile robot using genetic algorithms. *Information Sciences*. 2009;179:2158-74.
- [50] Wang S-Y, Liu F-Y, Chou J-H. Adaptive TSK fuzzy sliding mode control design for switched reluctance motor DTC drive systems with torque sensorless strategy. *Applied Soft Computing*. 2018;66:278-91.
- [51] Muñoz-Vázquez AJ, Gaxiola F, Martínez-Reyes F, Manzo-Martínez A. A fuzzy fractional-order control of robotic manipulators with PID error manifolds. *Applied Soft Computing*. 2019;83:105646.
- [52] Jahanshahi H, Yousefpour A, Wei Z, Alcaraz R, Bekiros S. A financial hyperchaotic system with coexisting attractors: Dynamic investigation, entropy analysis, control and synchronization. *Chaos, Solitons & Fractals*. 2019;126:66-77.
- [53] Ravandi AK, Khanmirza E, Daneshjou K. Hybrid force/position control of robotic arms manipulating in uncertain environments based on adaptive fuzzy sliding mode control. *Applied Soft Computing*. 2018;70:864-74.
- [54] Polák P, Jakša R, Vaščák J. Robotic attention manager using fuzzy controller with fractal analysis. *IEEE*. p. 002236-41.
- [55] Vascak J, Kovacik P, Hirota K, Sincak P. Performance-based adaptive fuzzy control of aircrafts. *IEEE*. p. 761-4.
- [56] Rajagopal K, Jahanshahi H, Varan M, Bayir I, Pham V-T, Jafari S, et al. A hyperchaotic memristor oscillator with fuzzy based chaos control and LQR based chaos synchronization. *AEU-International Journal of Electronics and Communications*. 2018;94:55-68.
- [57] Wang Y, Guan Z-H, Wen X. Adaptive synchronization for Chen chaotic system with fully unknown parameters. *Chaos, Solitons & Fractals*. 2004;19:899-903.
- [58] Shao S, Chen M, Yan X. Adaptive sliding mode synchronization for a class of fractional-order chaotic systems with disturbance. *Nonlinear Dynamics*. 2016;83:1855-66.
- [59] Petráš I. *Fractional-order nonlinear systems: modeling, analysis and simulation*: Springer Science & Business Media; 2011.
- [60] Ortigueira M, Machado J. Which derivative? *Fractal and Fractional*. 2017;1:3.
- [61] Ortigueira MD. On the “walking dead” derivatives: Riemann-Liouville and Caputo. *IEEE*. p. 1-4.
- [62] Magin RL. *Fractional calculus in bioengineering*: Begell House Redding; 2006.
- [63] Kilbas AAA, Srivastava HM, Trujillo JJ. *Theory and applications of fractional differential equations*: Elsevier Science Limited; 2006.
- [64] Trigeassou J-C, Maamri N, Oustaloup A. The infinite state approach: Origin and necessity. *Computers & Mathematics with Applications*. 2013;66:892-907.
- [65] Ortigueira MD, Machado JAT. What is a fractional derivative? *Journal of computational Physics*. 2015;293:4-13.
- [66] Ross B. A brief history and exposition of the fundamental theory of fractional calculus. *Fractional calculus and its applications*: Springer; 1975. p. 1-36.
- [67] Khalil R, Al Horani M, Yousef A, Sababheh M. A new definition of fractional derivative. *Journal of Computational and Applied Mathematics*. 2014;264:65-70.
- [68] Kiryakova V. A long standing conjecture failed. *Transform methods and special functions*, Varna. 1998;96:579-88.
- [69] Ortigueira MD. *Fractional calculus for scientists and engineers*: Springer Science & Business Media; 2011.
- [70] Brzeziński DW. Accuracy problems of numerical calculation of fractional order derivatives and integrals applying the Riemann-Liouville/Caputo formulas. *Applied Mathematics and Nonlinear Sciences*. 2016;1:23-44.
- [71] Tavazoei MS, Haeri M. A necessary condition for double scroll attractor existence in fractional-order systems. *Physics Letters A*. 2007;367:102-13.

- [72] Tavazoei MS, Haeri M. Chaotic attractors in incommensurate fractional order systems. *Physica D: Nonlinear Phenomena*. 2008;237:2628-37.
- [73] Wolf A, Swift JB, Swinney HL, Vastano JA. Determining Lyapunov exponents from a time series. *Physica D: Nonlinear Phenomena*. 1985;16:285-317.
- [74] Jarad F, Abdeljawad T, Baleanu D. Stability of q-fractional non-autonomous systems. *Nonlinear Analysis: Real World Applications*. 2013;14:780-4.
- [75] Chen D, Zhang R, Liu X, Ma X. Fractional order Lyapunov stability theorem and its applications in synchronization of complex dynamical networks. *Communications in Nonlinear Science and Numerical Simulation*. 2014;19:4105-21.
- [76] Li Y, Chen Y, Podlubny I. Stability of fractional-order nonlinear dynamic systems: Lyapunov direct method and generalized Mittag-Leffler stability. *Computers & Mathematics with Applications*. 2010;59:1810-21.
- [77] Zhang R, Liu Y. A new Barbalat's lemma and Lyapunov stability theorem for fractional order systems. *Control And Decision Conference (CCDC), 2017 29th Chinese: IEEE; 2017*. p. 3676-81.
- [78] Diethelm K. *The analysis of fractional differential equations: An application-oriented exposition using differential operators of Caputo type*: Springer Science & Business Media; 2010.
- [79] Li C, Deng W. Remarks on fractional derivatives. *Applied Mathematics and Computation*. 2007;187:777-84.
- [80] Lee H, Utkin VI. Chattering suppression methods in sliding mode control systems. *Annual reviews in control*. 2007;31:179-88.
- [81] Chen M, Chen WH. Sliding mode control for a class of uncertain nonlinear system based on disturbance observer. *International Journal of Adaptive Control and Signal Processing*. 2010;24:51-64.
- [82] Slotine J-JE, Li W. *Applied nonlinear control*: Prentice hall Englewood Cliffs, NJ; 1991.
- [83] Diethelm K, Ford NJ, Freed AD, Luchko Y. Algorithms for the fractional calculus: a selection of numerical methods. *Computer methods in applied mechanics and engineering*. 2005;194:743-73.